数理解析研究所講究録
第1847巻 2013年 73-85

Dynamics of the fluid balancer: Perturbation solution of a forced Korteweg-de Vries-Burgers equation

M. A. Langthjem[a]*, T. Nakamura[b]

[a] *Graduate School of Science and Engineering, Yamagata University, Jonan 4-chome, Yonezawa, 992-8510 Japan*

[b] *Department of Mechanical Engineering, Osaka Sangyo University, 3-1-1 Nakagaito, Daito-shi, Osaka, 574-8530 Japan*

Abstract

The work described here is concerned with the dynamics of a so-called fluid balancer; a hula hoop ring-like structure containing a small amount of liquid which, during rotation, is spun out to form a thin liquid layer on the outermost inner surface of the ring. The liquid is able to counteract unbalanced mass in an elastically mounted rotor. The present paper gives a detailed discussion of an approximate analytical solution which includes a so-called cnoidal wave; and it is demonstrated numerically how the surface wave can counterbalance the unbalanced mass.

Keywords: rotor, autobalancer, shallow water wave, cnoidal wave, forced Korteveg-de Vries-Burgers equation, method of multiple scales

1 Introduction

A fluid balancer is used in rotating machinery to eliminate the undesirable effects of unbalanced mass. It has become a standard feature in most household washing machines, but is also used in heavy industrial rotating machinery. Taking the washing machine fluid balancer as example, it consists of a hollow ring, like a hula hoop ring but typically with rectangular cross sections, which contains a small amount of liquid. The ring is typically attached on top of the drum. When it rotates at a high angular velocity Ω the liquid will form a thin liquid layer on the inner surface of the outermost wall, as sketched in Fig. 1.

Consider the situation where an unbalanced mass m is present, for example due to the non-uniform distribution of clothes in a washing machine. The rotor has a critical angular velocity Ω_{cr} where the centrifugal forces are in balance with the forces due to the restoring springs. Below this velocity ($\Omega < \Omega_{cr}$) the mass center of the fluid will be located 'on the same side' as the unbalanced mass, as shown in the left part of Fig. 1. [Here M indicates the mass of the

*[a]mikael@yz.yamagata-u.ac.jp, [b]t-nak@mech.osaka-sandai.ac.jp

empty rotor and $\mathcal{M}$ the mass of the contained liquid.] At a certain supercritical angular velocity $\Omega > \Omega_{cr}$ (say, during the spin drying process) the mass center of the liquid will move to the 'opposite side' of the unbalanced mass, as shown in the right part of Fig. 1, resulting in 'mass balance' and thus in reduced centrifugal forces and reduced oscillation amplitude of the rotor.

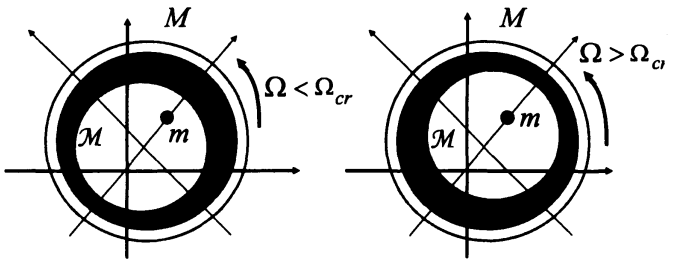

Figure 1: Working principle of the fluid balancer.

This is the working principle of the fluid balancer. The main idea appeared already in 1912, and US patent was granted in 1916 (Leblanc, 1916). The original layout consisted of one or several very narrow concentric channels (narrow in the radial direction but wide in the axial direction, i.e., perpendicular to the paper in Fig. 1) partially filled with, "liquid, or very small steel balls or metal fillings". Leblanc's fluid balancer was discussed and criticized by Thearle (1932); and later also by Den Hartog (1985), in connection with a discussion of Thearle's balancing head of 1932. It is argued there that Leblanc's balancer cannot work with a liquid, only with steel balls, and thus that the invention was flawed. It appears that this is due to the very narrow channels which basically prevent the formation of surface waves.

None the less, a complete automatic washing machine equipped with a fluid balancer was presented in 1940, and patented in 1945 (Dyer, 1945). The layout of the fluid balancer was very similar to the modern layouts, with a wide concentric channel, wide enough to allow for surface waves with large amplitudes.

The idea is thus not new; but recently there has been a renewed interest, both in industry and in academia. [There has also been a renewed interest in the so-called automatic dynamic balancer, as the balancer that uses steel balls running in a circular channel (or race) is called (van de Wouw *et al.*, 2005; Green *et al.*, 2006, 2008).]

Experimental fluid damper studies have been carried out by Kasahara *et al.* (2000a) and Nakamura (2009). As to mathematical models, simple lumped mass models have been considered by Bae *et al.* (2002), Jung *et al.* (2008), Majewski (2010), Chen *et al.* (2011), and Urbiola-Soto and Lopez-Parra (2011). The first and the last two of these papers include experimental studies as well. The paper by Jung *et al.* (2008) includes a few numerical simulation results based on computational fluid dynamics.

It should be emphasized that the fundamental principle of operation of the fluid balancer can be understood in terms of the explanation of Thearle's balancing head, given in Den Hartog (1985), p. 237. But a more detailed understanding is desirable; in particular, a more detailed understanding of the fluid dynamics of the balancer.

Good attention to fluid dynamic details has been given in many of the studies dealing with

the dynamics and stability of rotors partially filled with fluid/liquid; see e.g. Bolotin (1963) and Crandall (1995) for good overviews. Most of the studies, such as those of Wolf, Jr. (1968), Hendricks and Morton (1979) and Holm-Christensen and Träger (1991), are based on linear theory/linearization. While this is sufficient to determine the stability properties, it may be insufficient for modeling and understanding the dynamics of the fluid balancer (at any rate if free (unforced) wave components are included) since the amplitude of the surface waves need to be known.

Non-linear studies have been carried out by Berman *et al.* (1985), Colding-Jørgensen (1991), Kasahara *et al.* (2000b), and Yoshizumi (2007). Berman *et al.* (1985) found, both by numerical analysis and by experiment, that non-linear surface waves can exist on the fluid layer in the form of hydraulic jumps, undular bores, and ("what appears to be") solitary waves (or solitons). [An undular bore is a relatively weak hydraulic jump, with undulations behind it (Lighthill, 1978, p. 180). As to a solitary wave, described by the square of a hyperbolic secant function, sech, it should be noted that such a solution/wave exists only in a doubly infinite (i.e. non-periodic) domain. In the *periodic* domain of the rotor vessel, the solution which corresponds to a solitary wave is described by the square of a Jacobian elliptic cosine function, cn, and is termed a cnoidal wave.] Colding-Jørgensen (1991) concentrated on a hydraulic jump solution, following the analytical solution approach given in Berman *et al.* (1985). Contrary to this approach, the studies of Kasahara *et al.* (2000b) and Yoshizumi (2007) are purely numerical.

As by Colding-Jørgensen (1991) the formulation of the basic shallow water wave theory used in the present paper is based largely on the approach of Berman *et al.* (1985). The present work considers a rotor with two degrees of freedom, contrary to the one-degree-of-freedom assumption in Berman *et al.* (1985) and Colding-Jørgensen (1991). Also, rather than relying on a numerical integration approach, we find an (approximate) analytical solution to the fluid equations via a perturbation approach.

The present paper is to be considered as a continuation of Langthjem and Nakamura (2011) where the mathematical formulation of the problem is described in detail.

2 The fluid equations and approximate solution of them

The fluid motion in the rotating vessel is described by a shallow water approximation of the Navier-Stokes equations, and in terms of a coordinate system (x, y) attached to the wall of the rotor. This coordinate system is related to a polar coordinate system (r, θ) attached to the rotor such that $x = R\theta$, $y = R - r$, where R is the radius of the vessel. It is noted that x, y are rectangular (Cartesian) coordinates, indicating that curvature effects will be ignored. This is permissable when the fluid layer thickness $h(t, x)$ is sufficiently small in comparison with the vessel radius R, i.e., $|h(t, x)|/R \ll 1$ for all x, t. Under these assumptions the fluid equations of motion can be written as (Berman *et al.*, 1985; Whitham, 1999)

$$\frac{\partial u}{\partial t} + u\frac{\partial u}{\partial x} + v\frac{\partial u}{\partial y} - 2\Omega v = -\frac{1}{\rho}\frac{\partial p}{\partial x} + \nu\frac{\partial^2 u}{\partial y^2} + \mathfrak{F}, \tag{1}$$

$$\frac{\partial v}{\partial t} + 2\Omega u + R\Omega^2 = -\frac{1}{\rho}\frac{\partial p}{\partial y}. \tag{2}$$

Here u and v are the fluid velocity components in the x and y directions, p is the fluid pressure, ρ is the fluid density, ν is the kinematic viscosity of the fluid, and $\mathfrak{F}$ is a body force due to the rotating vessel.

A perturbation approach applied to (1) and (2) gives the following equation for the non-dimensional fluid layer perturbation $\kappa_0 = h'/R$ (with h' being the change in the fluid layer thickness h):

$$A_1\frac{\partial\kappa_0}{\partial\xi} - B_1\kappa_0\frac{\partial\kappa_0}{\partial\xi} - C_1\frac{\partial^3\kappa_0}{\partial\xi^3} - D_1\frac{\partial^2\kappa_0}{\partial\xi^2} + E_1\kappa_0^2 = x_*\sin\xi - y_*\cos\xi, \tag{3}$$

where A_1, B_1, D_1, and E_1 are parameters; see Langthjem and Nakamura (2011). The variable x_* and y_* represent the vessel deflections, and ξ is a 'traveling wave' variable, defined by $\xi = \frac{x}{R} - (\omega - \Omega)t$. Here ω is the angular whirling velocity of the vessel, which is assumed to be close, but not equal, to the imposed angular velocity Ω.

Equation (3) is a forced Korteweg-de Vries-Burgers equation. Without damping ($D_1 = E_1 = 0$) and external forcing ($x_* = y_* = 0$) it reduces to the classical Korteweg-de Vries equation. The Burgers equation is obtained with $C_1 = E_1 = 0$ (and again $x_* = y_* = 0$ too). A_1 is an unknown parameter which can be determined from the condition that the fluid volume must remain constant,

$$\Delta V_f = \int_0^{2\pi}\kappa_0(\xi)d\xi = 0. \tag{4}$$

2.1 Perturbation solution of the forced Korteweg-de Vries-Burgers equation (3)

Viscous wall friction is ignored in the following; that is, in (3) it will be assumed that $E_1 = 0$. The effect of this term is not uninteresting; but we are here mainly interested just in the qualitative aspects of the fluid balancer dynamics and wall friction is not considered to be essential in that respect.

When dividing through by C_1 (which is always $\neq 0$), (3) takes the form

$$a_1\frac{\partial\kappa_0}{\partial\xi} - b_1\kappa_0\frac{\partial\kappa_0}{\partial\xi} - \frac{\partial^3\kappa_0}{\partial\xi^3} + \varepsilon d_1\frac{\partial^2\kappa_0}{\partial\xi^2} = \varepsilon\left(\hat{x}\sin\xi - \hat{y}\cos\xi\right), \tag{5}$$

where

$$a_1 = \frac{A_1}{C_1}, \quad b_1 = \frac{B_1}{C_1}, \quad d_1 = \frac{D_1}{C_1}, \tag{6}$$

and

$$\hat{x} = \frac{x_*}{C_1}, \quad \hat{y} = \frac{y_*}{C_1}. \tag{7}$$

Here ε is a 'bookkeeping parameter' (order symbol) which is introduced to indicate the smallness of the rotor deflections $\hat{x}$, $\hat{y}$. The damping parameter d_1 is assumed to be of the same order of magnitude/smallness.

We seek an expansion on the form

$$\kappa_0(\xi) = v_0(\xi) + \varepsilon v_1(\xi) + \cdots \tag{8}$$

At the end of the analysis ε is set equal to one. It will be seen that any term contained in $v_1(\xi)$ will be proportional to either $\hat{x}$, $\hat{y}$, or d_1, which justifies this approach.

Inserting (8) into (5) we get

$$\varepsilon^0 \text{ order:} \quad a_1 \frac{\partial v_0}{\partial \xi} - b_1 v_0 \frac{\partial v_0}{\partial \xi} - \frac{\partial^3 v_0}{\partial \xi^3} = 0, \tag{9}$$

$$\varepsilon^1 \text{ order:} \quad a_1 \frac{\partial v_1}{\partial \xi} - b_1 \left(v_1 \frac{\partial v_0}{\partial \xi} + v_0 \frac{\partial v_1}{\partial \xi} \right) - \frac{\partial^3 v_1}{\partial \xi^3} - d_1 \frac{\partial^2 v_0}{\partial \xi^2} = \hat{x} \sin \xi - \hat{y} \cos \xi. \tag{10}$$

2.2 Cnoidal wave solution of (9)

Equation (9) is a Korteweg-de Vries equation which can be solved in exact, closed form. The solution is

$$v_0(\xi) = \alpha \mathrm{cn}^2 \left[\Xi \xi, k \right]. \tag{11}$$

Here cn is the Jacobian elliptic cosine function (Whittaker and Watson, 1927; Abramomitz and Stegun, 1965), with the parameters

$$\Xi = \left\{ \tfrac{1}{12} b_1 \left(2\alpha - 3\frac{a_1}{b_1} \right) \right\}^{\frac{1}{2}}, \quad k = \left\{ \frac{\alpha}{2\alpha - 3a_1/b_1} \right\}^{\frac{1}{2}}. \tag{12}$$

The solution (11) is called a cnoidal wave (due to the cn-function), and α is the amplitude of the wave. The parameter k is called the modulus (of the elliptic function).

The period of the function $\mathrm{cn}[\xi, k]$ is $4K$, where

$$K = K(k) = \int_0^{\frac{\pi}{2}} \left(1 - k^2 \sin^2 \theta \right)^{-\frac{1}{2}} \mathrm{d}\theta \tag{13}$$

is the complete elliptic integral of the first kind (Abramomitz and Stegun, 1965). Thus the period of $\mathrm{cn}^2[\xi, k]$ is $2K$, and the period (T_0, say) of the solution (11) is

$$T_0 = \frac{2K(k)}{\Xi} = 4K(k) \left\{ \frac{3}{b_1(2\alpha - 3a_1/b_1)} \right\}^{\frac{1}{2}}. \tag{14}$$

We seek a 2π-periodic solution, such that $\kappa_0(0) = \kappa_0(2\pi)$. Thus, one condition for determination of the two unknown parameters $\tilde{\omega}_1$ (which is hidden in a_1) and α is that

$$T_0(\tilde{\omega}_1, \alpha) = 2\pi, \qquad \text{or} \qquad \Delta T_0 = T_0(\tilde{\omega}_1, \alpha) - 2\pi = 0. \tag{15}$$

Another condition is that of conservation of fluid volume, as expressed by (4).

It is noted, finally, that the Jacobian elliptic cosine function cn degenerates into the hyperbolic secant function sech when $k \to 1$ and into the normal cosine function cos when $k \to 0$. Regarding the first case, it will be seen from (13) that $k \to 1$ implies that the $K \to \infty$, that is, the period goes towards infinity. The solution in this case ($\alpha \mathrm{sech}^2 [\Xi \xi]$) is known as a solitary wave, or a soliton.

2.3 Multiple scales solution of (10)

For the determination of $v_1(\xi)$, the second term in the expansion of $\kappa_0(\xi)$, we will make the assumption that the modulus k of $v_0(\xi)$ is small. The following expansion is then valid (Abramomitz and Stegun, 1965):

$$\mathrm{cn}[u, k] = \cos u + \tfrac{1}{4} k^2 (u - \sin u \cos u) \sin u + O(k^4) = \cos u + O(k^2). \tag{16}$$

Assuming here, for simplicity, that $|k| \ll 1$, we drop the $O(k^2)$ terms. That is, for the determination of $v_1(\xi)$, we assume that

$$v_0(\xi) \approx \alpha \cos^2 \Xi\xi = \tfrac{1}{2}\alpha \{1 + \cos 2\Xi\xi\}. \tag{17}$$

[It is noted here that in connection with the numerical examples to follow, it has been verified that k actually is small.]

Now, integration of (10) with respect to ξ gives

$$a_1 v_1 - b_1 v_0 v_1 - \frac{\partial^2 v_1}{\partial \xi^2} - d_1 \frac{\partial v_0}{\partial \xi} = -\hat{x}\cos\xi - \hat{y}\sin\xi + C_1, \tag{18}$$

where C_1 is an integration constant. We choose to set $C_1 = 0$ in order to get a periodic solution.

Inserting (17) into (18) gives, after reordering the terms,

$$\frac{d^2 v_1}{d\xi^2} + \left\{ \mathfrak{a}^2 + \frac{1}{2}\alpha b_1 (1 + \cos 2\Xi\xi) \right\} v_1 = \hat{x}\cos\xi + \hat{y}\sin\xi + \alpha d_1 \Xi \sin 2\Xi\xi, \tag{19}$$

where $\mathfrak{a}^2$ is written in place of $-a_1$. [It is noted also that we write $dv_1/d\xi$ in place of $\partial v_1/\partial\xi$ from now on.]

Equation (19) is a forced Mathieu equation. It is noted here that if we had used (11) directly in (18) instead of the approximation (17), the homogeneous version of (19) would be a Lamé equation. Exact solutions exist; these are termed Lamé functions and a considerable literature about them exist (Whittaker and Watson, 1927; Ince, 1940a,b, 1956). Still, to solve the non-homogenous Lamé equation, approximations (i.e., series expansions of Lamé functions) would be necessary. It seems simpler, and in place, to introduce simplifications at an earlier stage - already in the differential equation - as done above.

Now α, which appears in (11), is used in the role of a small parameter. Employing the method of multiple scales (Nayfeh, 2004), $v_1(\xi)$ is expanded as

$$v_1(\xi) = \sum_{m=0}^{M-1} \alpha^m \nu_m(\xi_0, \xi_1, \cdots, \xi_M), \tag{20}$$

where

$$\xi_0 = \xi, \quad \xi_1 = \alpha\xi, \quad \xi_2 = \alpha^2\xi, \cdots \tag{21}$$

It is noted that, while the final solution (20) will contain terms up to order $M-1$, the expansion must be carried out up to order M. We choose $M = 2$; thus

$$\frac{d\nu_m}{d\xi} = \frac{\partial \nu_m}{\partial \xi_0} + \alpha \frac{\partial \nu_m}{\partial \xi_1} + \alpha^2 \frac{\partial \nu_m}{\partial \xi_2} = D_0 \nu_m + \alpha D_1 \nu_m + \alpha^2 D_2 \nu_m. \tag{22}$$

Inserting (20) (running up to $M = 2$) and (22) into (19) gives

$$\varepsilon^0 \text{ order:} \quad D_0^2 \nu_0 + \mathfrak{a}^2 \nu_0 = \hat{x}\cos\xi_0 + \hat{y}\sin\xi_0, \tag{23}$$

$$\varepsilon^1 \text{ order:} \quad D_0^2 \nu_1 + \mathfrak{a}^2 \nu_1 = -2D_0 D_1 \nu_0 - \frac{b_1}{2}(1 + \cos 2\Xi\xi_0)\nu_0 + d_1 \Xi \sin 2\Xi\xi_0, \tag{24}$$

$$\varepsilon^2 \text{ order:} \quad D_0^2 \nu_2 + \mathfrak{a}^2 \nu_2 = -D_1^2 \nu_0 - 2D_0 D_2 \nu_0 - 2D_0 D_1 \nu_1 - \frac{b_1}{2}(1 + \cos 2\Xi\xi_0)\nu_1. \tag{25}$$

The complete solution to (23) is

$$\nu_0(\xi_0,\xi_1,\xi_2) = A(\xi_1,\xi_2)\mathrm{e}^{\mathrm{i}\mathfrak{a}\xi_0} + \frac{1}{2}\frac{\hat{x}-\mathrm{i}\hat{y}}{\mathfrak{a}^2-1}\mathrm{e}^{\mathrm{i}\xi_0} + \text{c. c.}, \tag{26}$$

where $A(\xi_1,\xi_2)$ is a complex function and c. c. denotes the complex conjugates of the preceeding terms. Inserting (26) into (24) gives

$$\begin{aligned} D_0^2\nu_1 + \mathfrak{a}^2\nu_1 = -\mathrm{e}^{\mathrm{i}\mathfrak{a}\xi_0}\left[2\mathrm{i}\mathfrak{a}D_1A + \frac{b_1}{2}\left(1+\cos 2\Xi\xi_0\right)A\right] - \frac{i}{2}d_1\Xi\mathrm{e}^{\mathrm{i}2\Xi\xi_0} \\ -\frac{b_1}{4}\frac{\hat{x}-\mathrm{i}\hat{y}}{\mathfrak{a}^2-1}\left[\mathrm{e}^{\mathrm{i}\xi_0} + \frac{1}{2}\mathrm{e}^{\mathrm{i}(1+2\Xi)\xi_0} + \frac{1}{2}\mathrm{e}^{\mathrm{i}(1-2\Xi)\xi_0}\right] + \text{c. c.} \end{aligned} \tag{27}$$

Secular terms will not appear in the solution to (27) if

$$2\mathrm{i}\mathfrak{a}D_1A + \frac{b_1}{2}\left(1+\cos 2\Xi\xi_0\right)A = 0. \tag{28}$$

Writing $A = \frac{1}{2}a\mathrm{e}^{\mathrm{i}\phi}$ and separating real and imaginary parts gives

$$\frac{da}{d\xi_1} = 0, \quad \frac{d\phi}{d\xi_1} = \frac{b_1}{4\mathfrak{a}}\left(1+\cos 2\Xi\xi_0\right). \tag{29}$$

These equations have the solutions

$$a = \hat{a}(\xi_2), \quad \phi = \frac{b_1}{4\mathfrak{a}}\left(1+\cos 2\Xi\xi_0\right)\xi_1 + \hat{\phi}(\xi_2) \tag{30}$$

With (28) being satisfied, a particular solution of (27) is

$$\begin{aligned} \nu_1 = -\frac{b_1}{4}\frac{\hat{x}-\mathrm{i}\hat{y}}{\mathfrak{a}^2-1}\left[\frac{\mathrm{e}^{\mathrm{i}\xi_0}}{\mathfrak{a}^2-1} + \frac{\mathrm{e}^{\mathrm{i}(1+2\Xi)\xi_0}}{2\{\mathfrak{a}^2-(1+2\Xi)\}} + \frac{\mathrm{e}^{\mathrm{i}(1-2\Xi)\xi_0}}{2\{\mathfrak{a}^2-(1-2\Xi)\}}\right] \\ -\frac{i}{2}\frac{d_1\Xi\,\mathrm{e}^{\mathrm{i}2\Xi\xi_0}}{\mathfrak{a}^2-4\Xi^2} + \text{c. c.} \end{aligned} \tag{31}$$

Next (26) and (31) are inserted into (25). This gives

$$\begin{aligned} D_0^2\nu_2 + \mathfrak{a}^2\nu_2 = \left[\frac{1}{2}\hat{a}(\xi_2)\left(\frac{b_1}{4\mathfrak{a}}\right)^2\left(1+\cos 2\Xi\xi\right)^2 - \mathfrak{a}\left\{\mathrm{i}\frac{da}{d\xi_2} - \hat{a}\frac{d\phi}{d\xi_2}\right\}\right] \times \\ \times \exp(\mathrm{i}\mathfrak{a}\xi_0)\exp(\mathrm{i}(\tfrac{b_1}{4\mathfrak{a}})(1+\cos 2\Xi\xi_0)\xi_1 + \hat{\phi}(\xi_2)) \\ +\text{n. s. t.} + \text{c. c.}, \end{aligned} \tag{32}$$

where n. s. t. stands for non-secular terms, that is, terms that are not proportional to $\exp(\mathrm{i}\mathfrak{a}\xi_0)$.

Secular terms will not appear in the solution to (32) if the terms in the square brackets on the right-hand side are equal to zero. This condition gives, upon separation of real and imaginary parts,

$$\hat{a}(\xi_2) = \bar{a}, \quad \hat{\phi}(\xi_2) = \frac{1}{2\mathfrak{a}}\left(\frac{b_1}{4\mathfrak{a}}\right)^2\left(1+\cos 2\Xi\xi\right)^2\xi_2 + \bar{\phi}, \tag{33}$$

where $\bar{a}$ and $\bar{\phi}$ are constants. For the final solution we will choose $\bar{a} = 0$ which will leave (11) as the only free (unforced) wave oscillation component in the final solution. Inserting these results into (26) and (31) and returning to the original variables we thus get

$$v_1(\xi) = \nu_0(\xi) + \alpha\nu_1(\xi) + O(\alpha^2) \tag{34}$$

with

$$\nu_0(\xi) = -\frac{1}{\mathfrak{a}^2 - 1}\{\hat{x}\cos\xi + \hat{y}\sin\xi\} \tag{35}$$

and

$$\begin{aligned}\nu_1(\xi) = &-\frac{b_1}{2}\frac{1}{(\mathfrak{a}^2-1)^2}\{\hat{x}\cos\xi + \hat{y}\sin\xi\} - \frac{b_1}{4}\frac{\hat{x}\cos\{(1+2\Xi)\xi\} + \hat{y}\sin\{(1+2\Xi)\xi\}}{(\mathfrak{a}^2-1)\{\mathfrak{a}^2-(1+2\Xi)^2\}} \\ &-\frac{b_1}{4}\frac{\hat{x}\cos\{(1-2\Xi)\xi\} + \hat{y}\sin\{(1-2\Xi)\xi\}}{(\mathfrak{a}^2-1)\{\mathfrak{a}^2-(1-2\Xi)^2\}} + \frac{d_1\Xi}{\mathfrak{a}^2-4\Xi^2}\sin 2\Xi\xi.\end{aligned} \tag{36}$$

The results given above are valid only when internal resonance does not take place, that is, when $\mathfrak{a}^2$ is away from 1. If $\mathfrak{a}^2$ is close to 1 then there are several special cases that need to be analyzed, such as Ξ close to 1, close to $\frac{1}{2}$, and Ξ away from these values. In the numerical work (to be described in the following) we have not experienced problems with proximity to an internal resonance. Accordingly those special cases will not be analyzed here.

3 Numerical evaluation approach

There are four unknown parameters in our problem, namely a frequency parameter $\tilde{\omega}_1$ included in the coefficient A_1, the amplitude parameter α defined by (11), and the rotor deflection components x_* and y_*. The four equations needed for determining these four parameters are (*i*, *ii*) the two coupled rotor equations of motion, (*iii*) the volume constraint specified by (4), and (*iv*) the periodicity constraint specified by (15). The unknown parameters are now determined as follows.

First guesses are made on the values of $\tilde{\omega}_1$ and α, in order to evaluate the fluid forces. [See Langthjem and Nakamura (2011) for the specific equations.] Then the rotor equation system is solved with respect to x_* and y_*. Following this, improved values of $\tilde{\omega}_1$ and α are obtained by taking one step with the Newton algorithm

$$\begin{Bmatrix}\tilde{\omega}_1\\ \alpha\end{Bmatrix}_{n+1} = \begin{Bmatrix}\tilde{\omega}_1\\ \alpha\end{Bmatrix}_n - \left(\frac{1}{D}\begin{bmatrix}\frac{\partial\Delta V_f}{\partial\alpha} & -\frac{\partial\Delta T_0}{\partial\alpha}\\ -\frac{\partial\Delta V_f}{\partial\tilde{\omega}_1} & \frac{\partial\Delta T_0}{\partial\tilde{\omega}_1}\end{bmatrix}\begin{Bmatrix}\tilde{\omega}_1\\ \alpha\end{Bmatrix}\right)_n, \quad D = \begin{vmatrix}\frac{\partial\Delta T_0}{\partial\tilde{\omega}_1} & \frac{\partial\Delta T_0}{\partial\alpha}\\ \frac{\partial\Delta V_f}{\partial\tilde{\omega}_1} & \frac{\partial\Delta V_f}{\partial\alpha}\end{vmatrix}. \tag{37}$$

Then the fluid forces are again evaluated and the rotor equation system is again solved with respect to x_* and y_*. This loop is continued until the absolute values of ΔV_f and ΔT_0, which should ideally be zero, are deemed sufficiently small, say smaller than 10^{-5}.

4 Numerical example

Vessel deflection components x_*, y_* and fluid force components F_x, F_y are shown in Fig. 2, parts (a) and (c). Here Ω_* is a non-dimensional vessel rotational speed, defined by $\Omega_* = \Omega/\omega_s$, with ω_s being the critical rotational speed for the empty rotor.

Part (b) and (d) show the phase angle of the vessel deflection (φ_d, say) and of the resultant fluid force (φ_f, say), respectively. The phase angle of the deflection starts, by small rotational speeds, at $\varphi_d \approx 0$; that is, the deflection is in the direction of the unbalanced mass. Upon passing through resonance the phase angle shifts approximately 180°. (By zooming in on the graph the precise value $\varphi_d = -177°$ is found.) The phase angle of the resultant fluid force (shown by a full line) has a similar course and ends, upon passing through resonance, at the value $\varphi_d = -190°$.

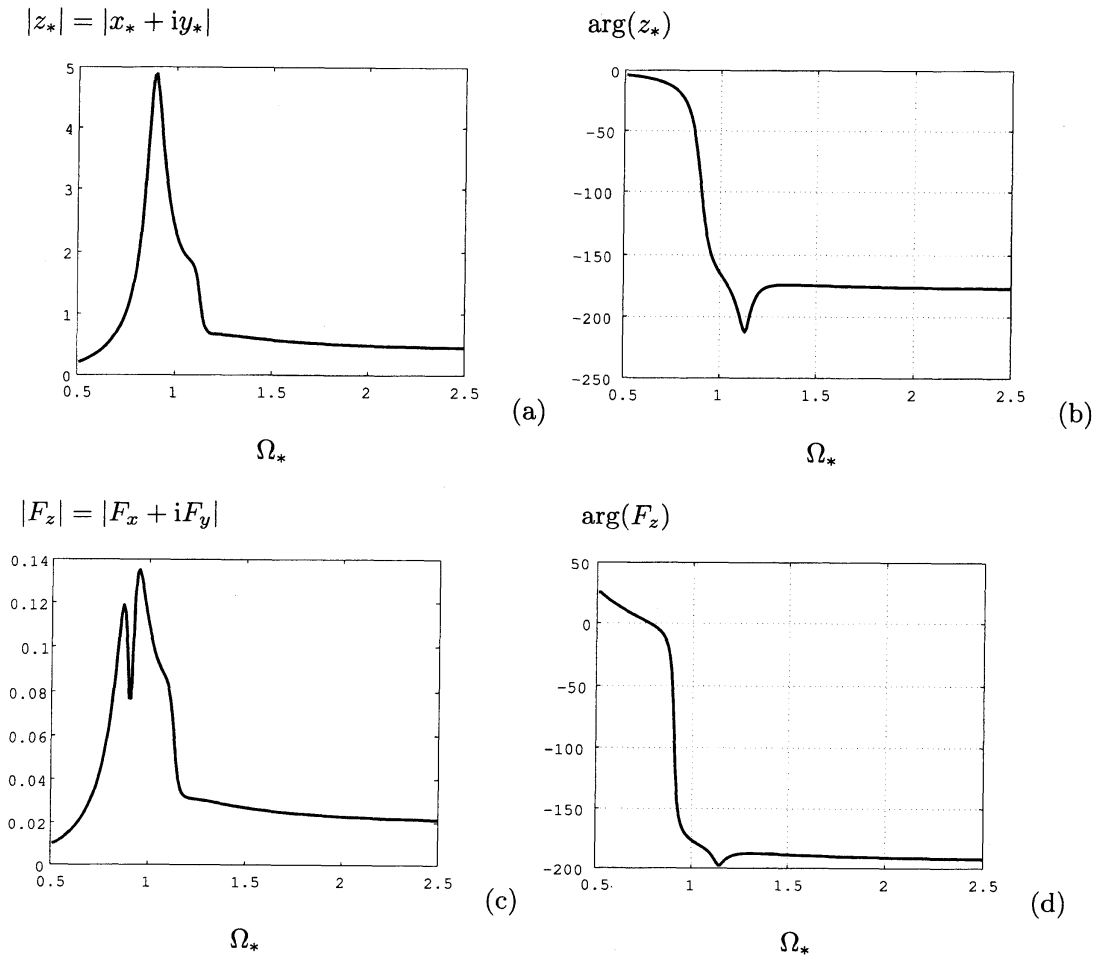

Figure 2: Vessel deflection and fluid force amplitudes (a, c) and phase angles (b, d; in degrees) as functions of the angular velocity Ω_*.

Thus, after the passage through resonance, the resultant fluid force starts to work against the unbalanced mass, tending to generate a deflection which is opposed to the deflection generated by the unbalanced mass. This explains the basic dynamics of the fluid balancer.

Fig. 3 shows the liquid surface, described by the non-dimensional parameters $\delta + \kappa_0$, for a sub-critical value of Ω_* ($\Omega_* = 0.6$) in parts (a) and (c); and for a super-critical value ($\Omega_* = 1.6$) in parts (b) and (d). [Parts (a) and (b) give an 'outfolded' representation in rectangular coordinates, while parts (c) and (d) give a more physical representation in polar coordinates.]

It is noted that 'unphysical' solutions can be generated around $\Omega_* \approx 1$, in the sense that $\delta + \kappa_0(\xi)$ (which should be > 0 for all ξ) can become < 0 at certain values of ξ. The problem has been reported and discussed also by Jung *et al.* (2008) and Urbiola-Soto and Lopez-Parra (2011). In order to avoid it, constraints on the form $\delta + \kappa_0(\xi) > 0$ should be imposed at a relatively large number of values of ξ around the circumference. This will imply that there will be (many) more equations than unknowns and will in turn require that the Newton method (37) is replaced by, for example, a least squares methodology. We prefer, however, to avoid this at the present stage. The issue does not cause any 'singular' behavior in the equation system and does not seem to cause qualitative changes in the frequency response diagrams either.

Returning to Fig. 3, initially (at time $t_* = 0$, say) the unbalanced mass is located at $\xi = 0$, in a coordinate system moving with the whirl (i.e., with the angular velocity $\omega - \Omega$, or $\tilde{\omega} - 1$ in terms of non-dimensional parameters). Thus, a wave top is located at the position of the unbalanced mass by the sub-critical rotational speed, and opposite of the unbalanced mass by the super-critical rotational speed, just as illustrated in Fig. 1. There is however a slow 'drift' with angular velocity $1 - \tilde{\omega}$. This undesirable phenomenon has been verified in experiments, and various remedies have been considered in order to prevent it, e.g. a hexagon-shaped channel and separator plates (Nakamura, 2009).

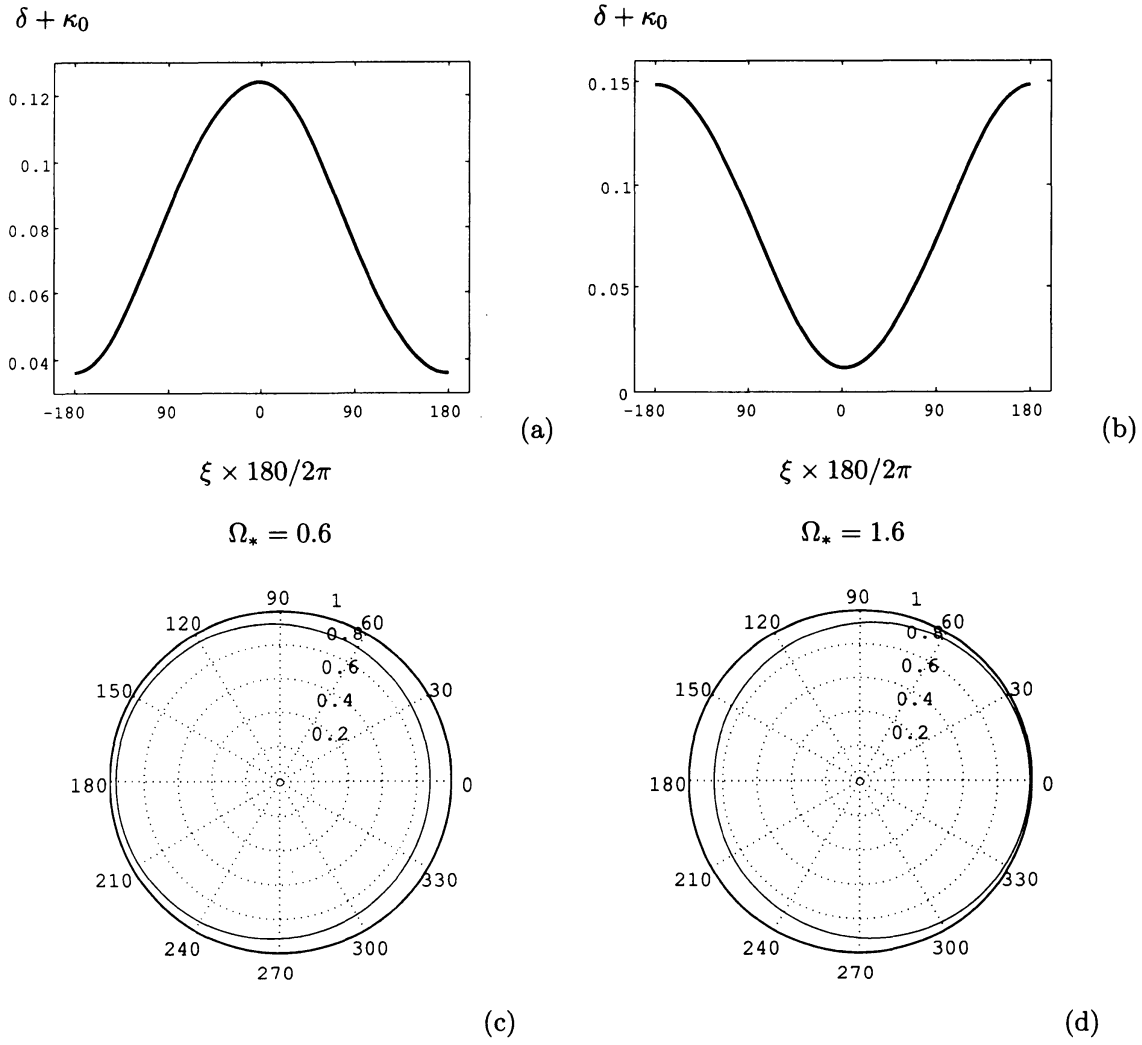

Figure 3: The fluid layer in the vessel, described by $\delta + \kappa_0$, in terms of 'rectangular' plots (a, b) and polar plots (c, d). The unbalanced mass is initially (at time $t_* = 0$, say) located at $\xi = 0$. Parts (a) and (c) show the fluid layer before resonance ($\Omega_* = 0.6$) and parts (b) and (d) the fluid layer after resonance ($\Omega_* = 1.6$).

5 Conclusion

The dynamics of the fluid balancer has been investigated based on a model of a two degrees-of-freedom rotor containing a small amount of liquid. The thin internal fluid layer, which forms due to the rotation, is described in terms of shallow water wave theory. A perturbation approach gives that the fluid layer thickness perturbation is described by a forced Korteweg-de Vries-Burgers equation. This equation is solved - approximately - also by a perturbation approach. The first approximation involves a (single) cnoidal wave solution of the (homogeneous) Korteweg-de Vries equation. The next term in the approximation is governed by a forced Mathieu equation.

The fluid and rotor equations are coupled by integrating the fluid pressure over the inner vessel surface. The phase angle function of the resultant fluid force has a behavior that resembles the experimentally obtained function (Nakamura, 2009). In particular, it is confirmed that, when the unbalanced mass initially is placed at the angular position $\varphi = 0$ (in a coordinate system moving with the whirl), the phase angle of the resultant fluid force moves from $\varphi = 0°$ at subcritical rotational speeds to $\varphi = 180°$ at supercritical speeds; that is, after passage through resonance. As observed in experiments, there is however a drift of the resultant fluid force.

Finally, it must be mentioned that it is not difficult to find parameter values where the present numerical approach does not convergence. This suggests that a *stable* one-wave solution does not exist (at those parameter values). Numerical simulations (Kasahara *et al.*, 2000b) suggest the existence of multi-wave solutions, still of solitary (or rather, cnoidal) wave type. It is known (Miura, 1976) that the Korteweg de-Vries equation (9) admits multiple-soliton solutions (in a doubly infinite domain). It would be interesting to pursue such analytical multi-wave solutions to the fluid balancer problem in future research.

References

Abramomitz, M. and Stegun, I. A. (1965). *Handbook of Mathematical Functions*. Dover Publications, Inc., New York.

Bae, S., Lee, J. M., Kang, Y. J., Kang, J. S., and Yun, J. R. (2002). Dynamic analysis of an automatic washing machine with a hydraulic balancer. *J. Sound Vib.*, **257**, 3–18.

Berman, A. S., Lundgren, T. S., and Cheng, A. (1985). Asyncronous whirl in a rotating cylinder partially filled with liquid. *J. Fluid Mech.*, **150**, 311–327.

Bolotin, V. V. (1963). *Nonconservative Problems of the Theory of Elastic Stability*. Pergamon Press, Oxford, UK.

Chen, H.-W., Zhang, Q., and Fan, S.-Y. (2011). Study on steady-state response of a vertical axis automatic washing machine with a hydraulic balancer using a new approach and a method for getting a smaller deflection angle. *J. Sound Vib.*, **330**, 2017–2030.

Colding-Jørgensen, J. (1991). Limit cycle vibration analysis of a long rotating cylinder partly filled with fluid. *J. of Eng. for Gas Turbines and Power*, **113**, 563–567.

Crandall, S. H. (1995). Rotor dynamics. In W. Kliemann and N. S. Namachivaya, editors, *Nonlinear Dynamics and Stochastic Mechanics*, pages 1–44. CRC Press, Boca Raton.

Den Hartog, J. P. (1985). *Mechanical Vibrations*. Dover Publications, Inc. [Orig. 4th Ed. by McGraw-Hill 1956], New York.

Dyer, J. B. (1945). Domestic appliance. U. S. Patent No. 2,375,635.

Green, K., Champneys, A. R., and Lieven, N. J. (2006). Bifurcation analysis of an automatic dynamic balancing mechanism for eccentric rotors. *J. Sound Vib.*, **291**, 861–881.

Green, K., Champneys, A. R., Friswell, M. I., and Muñoz, A. M. (2008). Investigation of a multi-ball, automatic dynamic ball balancing mechanism for eccentric rotors. *Phil. Trans. R. Soc. A*, **366**, 705–728.

Hendricks, S. L. and Morton, J. B. (1979). Stability of a rotor partially filled with a viscous incompressible fluid. *J. Appl. Mech.*, **46**, 913–918.

Holm-Christensen, O. and Träger, K. (1991). A note on rotor instability caused by liquid motions. *J. Appl. Mech.*, **58**, 804–811.

Ince, E. L. (1940a). ₁The periodic Lamé functions. *Proc. Roy. Soc. Edinburgh*, **60**, 47–63.

Ince, E. L. (1940b). ₂Further investigations into the periodic Lamé functions. *Proc. Roy. Soc. Edinburgh*, **60**, 83–99.

Ince, E. L. (1956). *Ordinary Differential Equations*. Dover Publications, Inc., New York.

Jung, C.-H., Kim, C.-S., and Choi, Y.-H. (2008). A dynamic model and numerical study on the liquid balancer used in an automatic washing machine. *J. Mech. Sci. Tech.*, **22**, 1843–1852.

Kasahara, M., Kaneko, S., Oshita, K., and Ishii, H. (2000a). Experiments of liquid motion in a whirling ring. In *Proceedings of the Dynamics and Design Conference 2000, 5-8 August 2000*, pages 1–6, Tokyo, Japan. Japan Soc. Mech. Eng.

Kasahara, M., Kaneko, S., and Ishii, H. (2000b). Sloshing analysis of a whirling ring. In *Proceedings of the Dynamics and Design Conference 2000, 5-8 August 2000*, pages 1–6, Tokyo, Japan. Japan Soc. Mech. Eng.

Langthjem, M. A. and Nakamura, T. (2011). Dynamics of the fluid balancer. *RIMS Kokyoroku*, **1761**, 140–150.

Leblanc, M. (1916). Automatic balancer for rotating bodies. U. S. Patent No. 1,209,730.

Lighthill, J. (1978). *Waves in Fluids*. Cambridge University Press, Cambridge, UK.

Majewski, T. (2010). Fluid balancer for a washing machine. In *Proceedings of the XVI International Congress*, pages 1–10. SOMIM (Society of Mechanical Engineers of Mexico).

Miura, R. M. (1976). The Korteweg-de Vries equation: A survey of results. *SIAM Review*, **18**, 412–459.

Nakamura, T. (2009). Study on the improvement of the fluid balancer of washing machines. In *Proceedings of the 13th Asia-Pacific Vibrations Conference, 22-25 November 2009*, pages 1–8. University of Canterbury, New Zealand.

Nayfeh, A. H. (2004). *Perturbation Methods*. Wiley-VCH Verlag, Weinheim.

Thearle, E. (1932). A new type of dynamic-balancing machine. *Trans. ASME*, **54**, 131–141.

Urbiola-Soto, L. and Lopez-Parra, M. (2011). Dynamic performance of the Leblanc balancer for automatic washing machines. *J. Vibr. Acoust.*, **133**, 041014–1 – 041014–8.

van de Wouw, N., van den Heuvel, M. N., Nijmeijer, H., and van Rooij, J. A. (2005). Performance of an automatic ball balancer with dry friction. *Int. J. Bifurcation and Chaos*, **15**, 65–82.

Whitham, G. B. (1999). *Linear and Nonlinear Waves*. Wiley-Interscience, New York.

Whittaker, E. T. and Watson, G. N. (1927). *A Course of Modern Analysis*. Cambridge University Press, Cambridge, UK.

Wolf, Jr., J. A. (1968). Whirl dynamics of a rotor partially filled with liquid. *J. Appl. Mech.*, **35**, 676–682.

Yoshizumi, F. (2007). Self-excited vibration analysis of a rotating cylinder partiall filled with liquid (Nonlinear analysis by shallow water theory). *Trans. Japan Society of Mech. Eng. (C)*, **73**(735), 28–37.